

## Quark production in high energy electron positron collisions: from strange to top

---

**Yuichi Okugawa,<sup>a,b,\*</sup> Adrian Irles,<sup>c,e</sup> Hitoshi Yamamoto,<sup>c,d</sup> François Richard<sup>a</sup> and Roman Pöschl<sup>a</sup>**

<sup>a</sup>Université Paris Saclay,  
Orsay, France

<sup>b</sup>Tohoku University,  
Sendai, Japan

<sup>c</sup>Instituto de Física Corpuscular (IFIC),  
Paterna, Spain

<sup>d</sup>Universitat de Valencia,  
Paterna, Spain

<sup>e</sup>Consejo Superior de Investigaciones Científicas (CSIC),  
Paterna, Spain

E-mail: [yuichi.okugawa@cern.ch](mailto:yuichi.okugawa@cern.ch), [adrian.irles@ific.uv.es](mailto:adrian.irles@ific.uv.es),  
[yhitoshi@epx.phys.tohoku.ac.jp](mailto:yhitoshi@epx.phys.tohoku.ac.jp), [richard@lal.in2p3.fr](mailto:richard@lal.in2p3.fr),  
[poeschl@lal.in2p3.fr](mailto:poeschl@lal.in2p3.fr)

The process  $e^+e^- \rightarrow q\bar{q}$  with  $q\bar{q} = s\bar{s}, c\bar{c}, b\bar{b}, t\bar{t}$  plays a central role in the physics programs of high energy electron-positron colliders operating from  $O(100 \text{ GeV})$  to  $O(1 \text{ TeV})$  center of mass energies. Furthermore, polarized beams as available at the International Linear Collider (ILC) are an essential input for the complete measurement of the helicity amplitudes that govern the production cross section. Quarks, especially the heaviers, are likely messengers to new physics and at the same time they are ideal benchmark processes for detector optimization. All four processes call for superb primary and secondary vertex measurements, a high tracking efficiency to correctly measure the vertex charge and excellent hadron identification capabilities. Strange, charm and bottom production are already available below the  $t\bar{t}$  threshold. We will show with detailed detector simulations of the International Large Detector (ILD) that production rate and the forward backward asymmetries of the the different processes can be measured at the 0.1% to 0.7% level and how systematic errors can be controlled to reach this level of accuracy. The importance of operating at different center of mass energies and the discovery potential in terms of Randall-Sundrum models with warped extra dimensions will be outlined.

*International Conference on High Energy Physics*  
06-13 July 2022  
Bologna, Italy

---

\*On behalf of the ILD Concept Group

\*Speaker

## 1. Introduction

One of the physics observations that is anticipated at the future lepton colliders is the measurement of the vector and axial electroweak coupling between neutral vector bosons ( $Z^0$  and  $\gamma$ , potentially  $Z'$ ) and a quark pair through the  $e^+e^- \rightarrow q\bar{q}$  process. In the current Standard Model (SM), there is no explanation for the mass hierarchy of fermions. However, many models for the physics Beyond Standard Model (BSM), such as the Randall-Sundrum model [1], offers predictions of the aforementioned couplings in order to explain the hierarchy problem. Since the couplings between the  $Z$  boson and fermion pairs depend on the fermion helicities, it is also important to apprehend the initial and final states of the particles. The experimental approach for the measurements of coupling between the  $Z$  boson and  $q\bar{q}$  ( $q = c, b$ ) was first made by LEP and SLC collaborations through  $e^+e^- \rightarrow c\bar{c}$  and  $e^+e^- \rightarrow b\bar{b}$  at the  $Z$ -pole [2]. In the experiment, one can determine the couplings by measuring the the forward and backward asymmetry ( $A_{FB}$ ) which is defined as:

$$A_{FB} = \frac{\sigma_F - \sigma_B}{\sigma_F + \sigma_B} \quad (1)$$

where  $\sigma_F$  ( $\sigma_B$ ) is the  $e^+e^- \rightarrow q\bar{q}$  cross section integrated over the forward (backward) hemisphere of the quark scattering angle  $\theta$ , with respect to the electron beam axis. These cross sections are determined from the polar angle of reconstructed track of  $q$  ( $\cos\theta_q$ ). Therefore, having a precise measurements of the forward and backward cross section lead to the precision measurements of the couplings. In this analysis, the experimental methods and precision level of coupling measurements at the next generation lepton collider is introduced to demonstrate its capability and sensitivities towards new physics, using the full detector simulation of  $e^+e^- \rightarrow s\bar{s}$ ,  $c\bar{c}$ ,  $b\bar{b}$  and  $t\bar{t}$ .

## 2. ILC & ILD

The International Linear Collider (ILC) [3] is the electron-positron collider which is expected to run at  $\sqrt{s} = 250$  GeV at its launch. It is 20 km in length and can be extended to 30 km for  $\sqrt{s} = 500$  GeV. One of the key features of the ILC is the well defined initial and final states of the colliding particles, since it can polarize both electron and positron beams. Such feature will enable the ILC to measure various physics observables to high precision, thus distinguishing theories on BSM (Fig.1). The International Large Detector (ILD) [5] is one of the detector concepts (along with

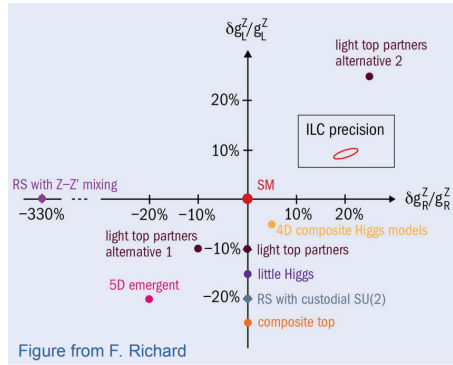


**Figure 1:** Predicted deviations of  $Z$  couplings to the left and right handed top quark [4]

SiD) that is proposed for the ILC. Its central trackers and highly granular calorimeters facilitates the high precision tracking and measurements of individual particles, which is achieved by the Particle Flow Algorithm, known as PFA [6]. PFA reconstructs Particle Flow Objects (PFO) of all particles within an event, identifying individual charged and neutral particles, including the constituents inside the jets.

### 3. Event Reconstruction

The events are generated using WHIZARD 1.95 [7], along with parton shower simulation is done by Pythia 6.422 [8]. The generated particles were then processed via full ILD GEANT4 detector simulation, which was used to produce the results shown here. A collision energy of  $\sqrt{s} = 250$  GeV was used for  $s\bar{s}$ ,  $c\bar{c}$ ,  $b\bar{b}$  production, and  $\sqrt{s} = 500$  GeV for  $t\bar{t}$  process. After the detector simulation process, jets were reconstructed using the Durham algorithm [9].

#### 3.1 Flavor Tagging

Powerful flavor tagging techniques are essential to be able to separate the different channels we are studying. Tagging of each jet requires a precise measurement of impact parameter since the long lived particles, such as  $b$  and  $c$  quark will decay at secondary vertices, the properties of which varies between different flavors. In the Figure 2, the tagging efficiency and purity of  $b$  and  $c$  tags in ILD are shown as a function of each flavor tagging cut. Their tagging performance shows their resilience towards other flavor backgrounds. After flavour tagging of the jets, the sum of the charges of PFOs associated to each secondary vertex is used to form the vertex charge. For the  $b\bar{b}$  and  $t\bar{t}$  process, this is the primary method to identify the generated quark charge, called *vertex method*.

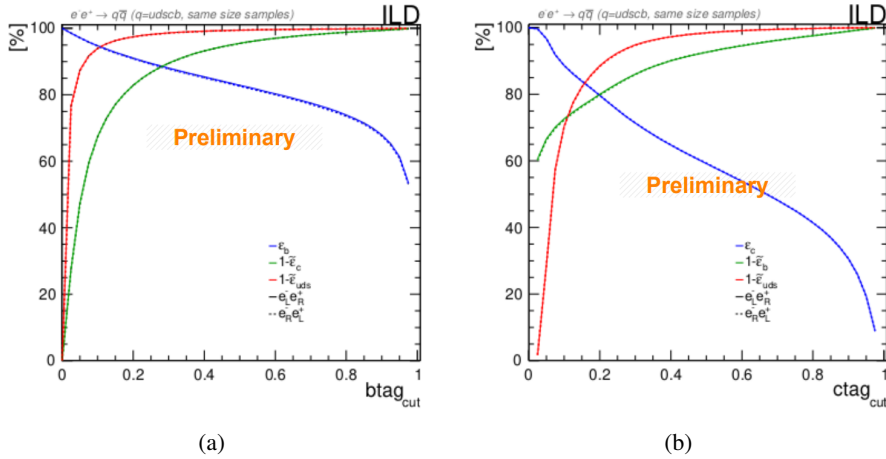


**Figure 2:** Flavor tagging performance for  $c$  (left) and  $b$  (right).  $\epsilon_c$  ( $\epsilon_b$ ) is the tagging efficiency after  $c$  ( $b$ ) tag cuts.  $1 - \tilde{\epsilon}_b$  ( $1 - \tilde{\epsilon}_c$ ) are the  $c$  ( $b$ ) tagging purity under  $b$  ( $c$ ) background.  $1 - \tilde{\epsilon}_{uds}$  is the flavor tagging efficiency under  $uds$  background. Finally, dotted and solid lines represent the same quantity with  $e_R^- e_L^+$  and  $e_L^- e_R^+$  beam polarization, respectively.

### 3.2 $dE/dx$ Measurements

Kaon identification can be the primary identifier for all flavors discussed in this analysis ( $s, c, b, t$ ) since they all could contain charged  $K$ :s at some point in their decay chain. The correct identification of the charged  $K$  is essentially to correctly assign the  $K$  to the quark or anti-quark of the underlying hard process. The stopping power  $dE/dx$  depends on the particle mass and velocity. It is measured by the Time Projection Chamber (TPC) of the ILD. For the particle identification,  $dE/dx$  distance is defined as follows:

$$dE/dx \text{ distance} = \text{sign}(dE/dx - dE/dx_{exp-Bethe}) \left[ \left( \frac{(dE/dx - dE/dx_{exp-Bethe})}{\Delta_{dE/dx}} \right)^2 \right] \quad (2)$$

where  $dE/dx_{exp-Bethe}$  is  $dE/dx$  value expected from Bethe-Bloch formula and  $\Delta_{dE/dx}$  is the statistical error for  $dE/dx$  measurements. At the current working point, purity (efficiency) for  $K$  identification using this method is 90 % (80 %), for the track momentum above 3 GeV. Quark charge identification using  $dE/dx$  distance is called *Kaon method*.

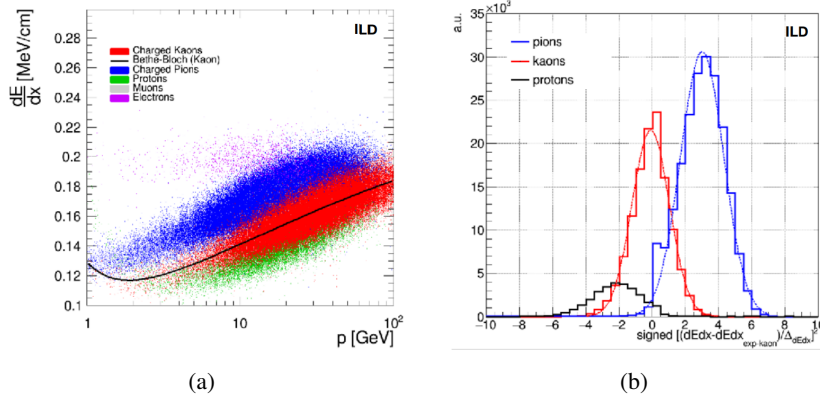


**Figure 3:** (a)  $dE/dx$  vs. momentum for each particle ( $e, \mu, K^\pm, p, \pi$ ). (b)  $dE/dx$  distances from kaon Bethe-Bloch formula.

### 4. Asymmetry Measurements

As discussed in Section 1, particle charge measurement is the key to precisely measure  $A_{FB}$ . For this analysis, integrated luminosities of  $4,600 \text{ fb}^{-1}$  was taken for  $s\bar{s}$  process,  $900 \text{ fb}^{-1}$  for  $c\bar{c}$  and  $b\bar{b}$  process, and  $3,200 \text{ fb}^{-1}$  for  $t\bar{t}$  process. The polar angle distribution is the vital information for seeking the asymmetry parameter. In Figure 4, polar angle distribution for four different processes is shown for the configuration  $e_L^- e_R^+$  of the beam polarization. Superimposed is a fit inspired by the differential cross section and defined as:

$$\frac{d\sigma}{d\cos\theta} = S \times (1 + \cos^2\theta) + A \times \cos\theta \quad (3)$$

where  $S$  and  $A$  are the parity conserving and parity violation coefficients of the differential cross sections, respectively. For all processes, the generated distribution of the hard process can be well reproduced after reconstruction in the angular range  $|\cos\theta| < 0.8$ . For the three lighter quarks, a drop in reconstruction efficiency is observed outside this range.

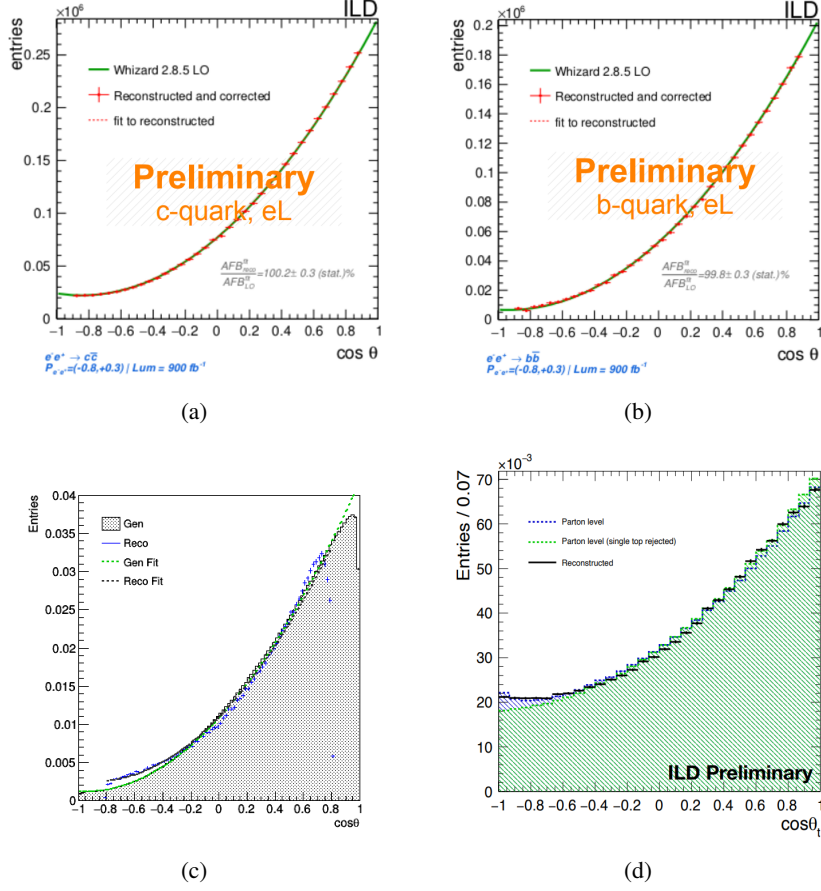


**Figure 4:** Reconstructed and generated polar angle distributions of the process (a)  $c\bar{c}$ , (b)  $b\bar{b}$ , (c)  $s\bar{s}$ , and (d)  $t\bar{t}$ . Superimposed is a fit inspired by the differential cross section. (see text for details)

## 5. Systematic and Statistical Uncertainties

Table 1 shows the expected statistical and systematic uncertainties of AFB for the processes  $e^+e^- \rightarrow c\bar{c}$  [10],  $e^+e^- \rightarrow b\bar{b}$  [11] and  $e^+e^- \rightarrow t\bar{t}$  [12]. The following sources of the systematic uncertainties have been taken into account: (a) flavor tagging and charge tagging (b) event selection including rejection of ISR events (c) event polarisation. QCD effects will be scrutinised in future studies. The accuracy here can open the sensitivity towards the measurements for the couplings to the propagators from new boson predicted in BSM theories.

	stat. / syst.		stat.
	$c\bar{c}$	$b\bar{b}$	$t\bar{t}$
$\Delta A_{FB}(e_L^- e_R^+)$	$\pm 0.16\% \pm 0.09\%$	$\pm 0.15\% \pm 0.13\%$	$\pm 0.70\%$
$\Delta A_{FB}(e_R^- e_L^+)$	$\pm 0.20\% \pm 0.10\%$	$\pm 0.15\% \pm 0.095\%$	$\pm 0.53\%$

**Table 1:** Statistical and systematic uncertainties for three different processes with different beam polarization.

## 6. Conclusion

In this paper, the analysis methods for  $e^+e^- \rightarrow q\bar{q}$  at the ILC were outlined. Quark pair production with four different flavors ( $s\bar{s}$ ,  $c\bar{c}$ ,  $b\bar{b}$ ,  $t\bar{t}$ ) were generated with full detector simulation of the ILD Detector Concept. Vertex charge and  $dE/dx$  distance measurements were used to identify the quark charge and as a result, their reconstructed polar angle distribution showed good agreement with generated distribution. Moreover, flavor tag studies from  $c\bar{c}$  and  $b\bar{b}$  analyses demonstrated high performance in both efficiency and purity.

## References

- [1] L. Randall and R. Sundrum, *A Large mass hierarchy from a small extra dimension*, *Phys. Rev. Lett.* **83** (1999) 3370 [[hep-ph/9905221](#)].
- [2] ALEPH, DELPHI, L3, OPAL, SLD, LEP ELECTROWEAK WORKING GROUP, SLD ELECTROWEAK GROUP, SLD HEAVY FLAVOUR GROUP collaboration, *Precision electroweak measurements on the Z resonance*, *Phys. Rept.* **427** (2006) 257 [[hep-ex/0509008](#)].
- [3] T. Behnke et al., *The International Linear Collider Technical Design Report - Volume 1: Executive Summary*, [1306.6327](#).
- [4] F. Richard, *Present and future constraints on top EW couplings*, [1403.2893](#).
- [5] H. Abramowicz et al., *The International Linear Collider Technical Design Report - Volume 4: Detectors*, [1306.6329](#).
- [6] M. Thomson, *Particle flow calorimetry and the pandorapfa algorithm*, *Nuclear Instruments and Methods in Physics Research Section A: Accelerators, Spectrometers, Detectors and Associated Equipment* **611** (2009) 25.
- [7] W. Kilian, T. Ohl and J. Reuter, *WHIZARD: Simulating Multi-Particle Processes at LHC and ILC*, *Eur. Phys. J. C* **71** (2011) 1742 [[0708.4233](#)].
- [8] T. Sjöstrand, S. Ask, J. R. Christiansen, R. Corke, N. Desai, P. Ilten et al., *An introduction to PYTHIA 8.2*, *Comput. Phys. Commun.* **191** (2015) 159 [[1410.3012](#)].
- [9] S. Catani, Y. Dokshitzer, M. Olsson, G. Turnock and B. Webber, *New clustering algorithm for multijet cross sections in  $e^+e^-$  annihilation*, *Physics Letters B* **269** (1991) 432.
- [10] A. Irlles, R. Pöschl and F. Richard, *Production and measurement of  $e^+e^- \rightarrow c\bar{c}$  signatures at the 250 gev ilc*, 2020.
- [11] ILD collaboration, *Determination of the electroweak couplings of the 3rd generation of quarks at the ILC*, *PoS EPS-HEP2019* (2020) 624.
- [12] ILD CONCEPT GROUP collaboration, *International Large Detector: Interim Design Report*, [2003.01116](#).